MINERAL MAPPING OF DRILL CORE HYPERSPECTRAL DATA WITH EXTREME LEARNING MACHINES

Cecilia Contreras, Mahdi Khodadadzadeh, Pedram Ghamisi, and Richard Gloaguen

Helmholtz-Zentrum Dresden-Rossendorf (HZDR),
Helmholtz Institute Freiberg for Resource Technology, Germany

ABSTRACT

Hyperspectral scanners are increasingly being used in the mining industry as a non-destructive and non-invasive technique to efficiently map minerals in drill core samples. Hyperspectral data allows the characterization of different mineral assemblages, structural features and alteration patterns based on reflectance spectrum profiles. Traditional methods to analysis drill core hyperspectral data include the use of reference spectral libraries by visual analysis or a well established software. However, although these approaches produce good results, they are time-consuming and prone to errors. Therefore, in this paper, we take advantage of the latest and advanced machine learning techniques proposed in different scientific fields and explore the use of extreme learning machines (ELM) to map minerals in drill core hyperspectral data. This is a supervised technique that provides fast and automatic means to characterize hyperspectral data. To be able to implement this technique, a reference map was generated from the drill core hyperspectral data. The obtained results indicate that ELM can successfully map minerals in drill core hyperspectral data producing better quantitative and qualitative results than a typical RF classifier.

Index Terms— Drill cores, hyperspectral data, mineral mapping, extreme learning machine, random forest.

1. INTRODUCTION

Drill core hyperspectral scanning is an emerging technique in the mining industry for the exploration of mineral deposits. Hyperspectral sensors record relevant spectral information through a wide range of wavelengths in several tens of spectral bands. The reflectance spectrum profiles in hyperspectral data cubes can be effectively exploited to characterize different minerals [1,2]. The hyperspectral drill core scanners offer an non-invasive and non-destructive technique for economical mineralogical analysis. More importantly, such analysis can be achieved in a fast turn-around time for a large amount of drill cores [3]. One of the most important tasks of hyperspectral drill core analysis is to determine the spatial distribution of minerals over the drill cores. This task is commonly known as mineral mapping.

Traditional approaches to map minerals in drill core hyperspectral data rely on the visual interpretation of the spectra and performing a comparison with the reference spectral libraries (e.g., USGS Spectral library [4]). For example, the Spectral Angle Mapper (SAM) has been frequently used to find the best match between the unknown hyperspectral pixels and the reference spectra [5, 6]. Taking different approaches in [7], Kruse *et al.* first made use of the Minimum Noise Fraction transformation (MNF) [8, 9], the Pixel Purity Index (PPI), and n-Dimensional visualizer for the selection of the endmembers [7]. Then, they visually analyzed and compared the selected endmembers to reference spectra for their identification. These endmembers were then used with the Mixture Tune Matched Filtering (MTMF) technique to produce mineral maps and partial abundances [10, 11]. More recently in [12], Mathieu *et al.* proposed to use different attributes of the absorption features after applying the MNF transformation to the mosaic of several drill core hyperspectral images. They mapped minerals based on the combination of the position and depth of the absorption features, which were selected after a visual analysis of the spectra using reference spectral libraries.

Lately, machine learning algorithms have been introduced in different scientific fields to improve the accuracy, speed, and robustness of data analysis. These techniques offer automatic means to discover underlying relations within large data sets [13]. Several techniques have been proposed in the literature, such as support vector machines (SVM) [14], random forest (RF) [15], and neural networks (NN) [16]. Recently, advanced NN-based techniques are increasingly being used specially for non-linearly separable data. Among different NN architectures, single layer feed-forward networks (SLFN) are the most commonly adopted ones. However, most of the existing learning algorithms used to train an SLFN do not guarantee a global optimal solution, especially when the parameters of the network are not properly fine-tuned [17]. To tackle this issue, extreme learning machines (ELM) algorithm has been recently proposed [18]. The hidden layer in the ELM algorithm is not required to be iteratively tuned and randomly fixed. Moreover, it has been shown that ELM networks are accurate and less computationally complex while providing comparable results with state-of-the-art algorithms [13].

Similar to other scientific fields, exploiting machine learning techniques for geological applications is also growing (see e.g., [19]). However, the use of machine learning techniques for drill core hyperspectral data analysis has not been well addressed in the literature. This is mainly due to the fact that in such data, defining meaningful classes and selecting representative training samples required for the training phase of a machine learning algorithm is not straightforward. Therefore, in this paper, we present a drill core data set, which include hyperspectral data and a reference map generated with the help of geologists. Then, we explore the capability of machine learning techniques for mineral mapping using this dataset. For the first time, we evaluate the ELM technique for the analysis of drill core hyperspectral data quantitatively and qualitatively. ELM is known for being remarkable efficient in terms of accuracy and computational complexity [13]. For comparison, we also explore the application of the traditional RF classifier for mineral mapping.

The rest of the paper is structured as follows: section 2 describes the used ELM. Section 3 presents data description, experimental results, and discussions. Finally, the conclusions are drawn in Section 4.

2. METHODOLOGY

We propose to use ELM to map minerals in drill core hyperspectral data (see Fig. 1). After the acquisition of the hyperspectral data, a reference map was generated by a geologist. This reference data was used as the training and test samples for the ELM technique. ELM is considered as the generalization of SLFN. However, in contrast with traditional training methods for the SLFN (i.e., iterative gradient-based learning approaches), the idea in ELM is to reach the smallest training error and the smallest norm of the weights [20]. The training of ELM consists of two stages: (1) the hidden layer is constructed by using a fixed number of randomly generated mapping neurons, and (2) the output weights are solved by minimizing the sum of the squared losses of the prediction errors. In this way, by fixing the input weights $\mathbf{w}_i = [w_{i1}, w_{i2}, \cdots, w_{id}]^T$, which connect the ith hidden node with the input nodes, and by fixing the hidden layers biases b_i, the only parameters that need to be optimized in the training process are the output weights between the hidden neurons and the output nodes. By doing so, SLFN can be trained in a similar manner to solve a regularized least-squares problem $\hat{\beta}$ of the linear system $\mathbf{H}\beta = \mathbf{Y}$ where $\mathbf{H}$ and β are the output matrix of the hidden layer and the output weight matrix, respectively. $\mathbf{Y}$ is the output matrix.

$$\text{Minimize:} \|\mathbf{H}\beta - \mathbf{Y}\|^2 \qquad \text{s.t.} \quad \|\beta\|^2.$$

Let $\{(\mathbf{x}_i, \mathbf{y}_i)\}_{i=1}^n$ be n distinct training samples, where, $\mathbf{x}_i = [x_{i1}, x_{i2}, \cdots, x_{id}]^T \in \mathbb{R}^d$ and $\mathbf{y}_i = [y_{i1}, y_{i2}, \cdots, y_{iK}]^T \in \mathbb{R}^K$. Here, d is the spectral dimension of the data and K is the number of classes. Moreover, let $\mathbf{h}(\mathbf{x})$ be $[f(\mathbf{w}_1 \cdot \mathbf{x} + b_1), ..., f(\mathbf{w}_L \cdot \mathbf{x} + b_L)]$, where $f(\mathbf{w}_i \cdot \mathbf{x} + b_i)$ is the output of the ith hidden node having the input sample $\mathbf{x}$. Then, from the theory of optimization, the previously presented minimization problem can be reformulated:

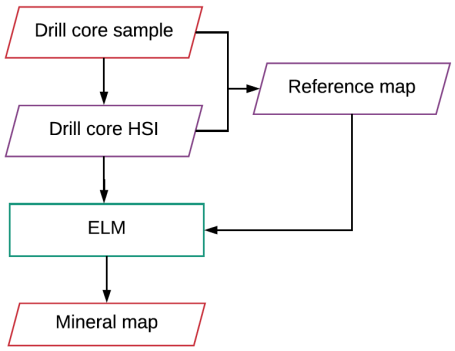

Fig. 1. Flowchart of the proposed technique to map minerals in drill core hyperspectral data. HSI stands for hyperspectral image and ELM for extreme learning machine.

$$\min_\beta \frac{1}{2}\|\beta\|_2^2 + C\frac{1}{2}\sum_{i=1}^{n}\xi_i^2,$$

$$\text{s.t.} \quad \mathbf{h}(\mathbf{x}_i)\beta = \mathbf{y}_i^T - \xi_i^2, \quad i = 1, \cdots, n,$$

where ξ_i^2 is the training error of the training sample $\mathbf{x}_i$, and C is a regularization parameter. Finally, the output of ELM can then be estimated as follows:

$$\mathbf{f}(\mathbf{x}) = \mathbf{h}(\mathbf{x})\beta = \mathbf{h}(\mathbf{x})\mathbf{H}^T(\frac{\mathbf{I}}{C} + \mathbf{H}\mathbf{H}^T)^{-1}\mathbf{Y}. \qquad (1)$$

3. EXPERIMENTAL RESULTS

To evaluate the performance of ELM, we acquired the hyperspectral data from the unpolished half of the drill core sample (see the *RGB image of the drill core* in Fig. 2). For the acquisition, we used a SisuRock drill core scanner equipped with an AisaFenix VNIR-SWIR hyperspectral sensor. The spectral range of the camera covers from 380 to 2500 nm, with a spectral resolution of 3.5 nm in the VNIR and 12 nm in the SWIR. The total number of bands is 450 and the pixel size is 1.5 mm/pixel. For the pre-processing of the data, first, radiometric and geometric corrections were carried out to correct the sensor shift and the effect of lenses, respectively. For this, we used the toolbox presented in [21]. To avoid bands with little or no coherence information, the data were spectrally excluded from 380 nm to 538 nm and from 2486 nm to 2500 nm. The resultant wavelength range covers from 538 nm to 2486 nm in 400 bands.

A reference map was generated by an expert based on an exhaustive visual analysis of the entire drill core sample and

its hyperspectral data. This reference map consists of the labeled samples and allows the use of supervised classification techniques. In general, the matrix in the sample is dominantly composed of feldspars and partly altered to white mica, chlorite, and biotite. Two main vein types are presented, one consisting of quartz and white mica and the other one consisting of gypsum, white mica, and scarce pyrite. Hence, four classes were considered enough to describe the drill core sample: *White mica*, *Gypsum*, *Chlorite*, and *Biotite*. Each pixel was assigned to the most dominant mineral class and no class label was assigned to these pixels in which the dominant mineral was not detectable (see *reference map* in Fig. 2).

For the ELM classifier, the number of nodes L was fixed to 1000 and the regularization parameter C was set in range of $C = 1, 10^1, \cdots, 10^5$ using five fold cross validation. To train the algorithm, we used 10% of the available samples in the reference map. The remaining samples were used as the test set. The total number of pixels available per class for the training and test sets are shown in Table 1. All the experiments were repeated 30 times and the mean of the the class accuracy, overall and average accuracies, and kappa coefficients are reported in Table 2. To better assess the performance of ELM when mapping minerals, the results of using the RF classifier are also reported. For this classifier, we considered an ensemble of 500 decision tree classifiers.

Several conclusions can be obtained from the experiments reported in Table 2. First and foremost, it is noticeable that, in general, the ELM technique outperforms the RF method. More specifically compared to the RF method, the ELM obtained 5.1% and 8.9% higher overall and average accuracies, respectively. Moreover, based on the variability of the overall and average accuracies provided by the standard deviation, it is evident that ELM produces more stable results than RF. In ELM, the overall and average accuracies fluctuate only by 0.5% and 1.7%, respectively, whereas in RF the variation ranges by 0.9% and 3.1%.

If we focus on the class specific accuracies, we can see that for the three main classes *Wmca*, *Gp*, and *Chl* the accuracies obtained by the ELM are higher than the RF. For instance, the *Gp* class accuracy resulted by the ELM technique is 44.9% higher than the one obtained by the RF method. However, for the *Bt* class, the RF obtained higher accuracy than the ELM, which can be considered to be the influence of the mixed characteristics of the matrix. Qualitatively, from the *ELM mineral map* and the *RF mineral map* in Fig. 2, it can be seen that although RF mapped scarce *Bt* content, the *Gp* content in the veins has not accurately mapped. However, the mineral map obtained by ELM shows less *Bt* content in the matrix but very well mapped *Gp* in the veins.

4. CONCLUSIONS AND REMARKS

In this paper, we use ELM to map minerals in drill core hyperspectral data. The ELM technique is highly efficient in terms of accuracy and computational complexity. Moreover, the hidden layer is fixed and it is not needed to be iteratively tuned. From the analysis of the results, we have seen that ELM provides better classification results than RF in terms of accuracies as well as qualitatively. Especially, ELM performs better than RF when the materials are not highly mixed.

As part of our future developments, we will optimize ELM and test different feature extraction techniques to be used as input for classifiers since we want to increase the accuracy and robustness for the mineral mapping task.

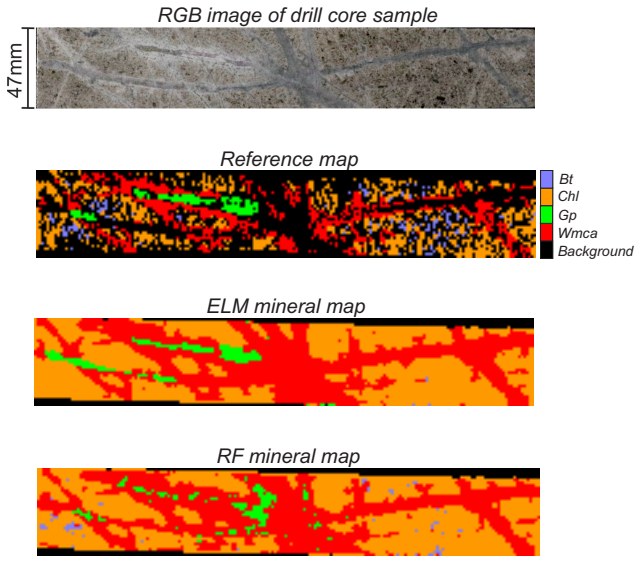

Fig. 2. The classification results of the drill core sample obtained by ELM and RF. Mineral abbreviations after [22].

Table 1. Total number of samples available in the reference data.

Class	Total	Training	Test
Wmca	993	99	894
Gp	151	15	136
Chl	1088	108	980
Bt	155	15	140

Table 2. Classification accuracies per class (in %), overall accuracy (in %), average accuracy (in %), and kappa coefficient (is of no unit). Accuracy values are reported in percentages.

Class	ELM	RF
Wmca	96.6	92.6
Gp	80.6	35.7
Chl	96.7	93
Bt	5	21.7
Overall	89.7 ($\pm$ 0.5)	84.6 ($\pm$ 0.9)
Average	69.7 ($\pm$ 1.7)	60.8 ($\pm$ 3.1)
Kappa	0.8226	0.7356

5. REFERENCES

[1] R. N Clark, "Spectroscopy of rocks and minerals, and principles of spectroscopy," in *Remote sensing for the earth sciences: Manual of remote sensing*, vol. 3, pp. 3–58. John Wiley & Sons, Inc, 1999.

[2] F. van der Meer, "Analysis of spectral absorption features in hyperspectral imagery," *International Journal of Applied Earth Observation and Geoinformation*, vol. 5, no. 1, pp. 55–68, 2004.

[3] F. A. Kruse, "Identification and mapping of minerals in drill core using hyperspectral image analysis of infrared reflectance spectra," *International Journal of Remote Sensing*, vol. 17, no. 9, pp. 1623–1632, 1996.

[4] Philip R. Christensen, Joshua L. Bandfield, Victoria E. Hamilton, Douglas A. Howard, Melissa D. Lane, Jennifer L. Piatek, Steven W. Ruff, and William L. Stefanov, "A thermal emission spectral library of rock-forming minerals," *Journal of Geophysical Research: Planets*, vol. 105, no. E4, pp. 9735–9739, 2000.

[5] Wendy M. Calvin and Elizabeth L. Pace, "Mapping alteration in geothermal drill core using a field portable spectroradiometer," *Geothermics*, vol. 61, pp. 12–23, 2016.

[6] E Littlefield, W Calvin, P Stelling, and T Kent, "Reflectance spectroscopy as a drill core logging technique: An example using core from the Akutan," *Geothermal Resources Council Annual Meeting 2012 - Geothermal: Reliable, Renewable, Global, GRC 2012*, vol. 36 2, no. 2011, pp. 1281–1283, 2012.

[7] F. A. Kruse, R. L. Bedell, J. V. Taranik, W. A. Peppin, O. Weatherbee, and W. M. Calvin, "Mapping alteration minerals at prospect, outcrop and drill core scales using imaging spectrometry," *International Journal of Remote Sensing*, vol. 33, no. 6, pp. 1780–1798, 2012.

[8] A. J. Mauger, J. L. Keeling, and J. F. Huntington, "Alteration mapping of the Tarcoola Goldfield (South Australia) using a suite of hyperspectral methods," *Applied Earth Science*, vol. 116, no. 1, pp. 2–12, 2007.

[9] Elizabeth F. Littlefield and Wendy M. Calvin, "Geothermal exploration using imaging spectrometer data over Fish Lake Valley, Nevada," *Remote Sensing of Environment*, vol. 140, pp. 509–518, 2014.

[10] E. Bedini, F. van der Meer, and F. van Ruitenbeek, "Use of HyMap imaging spectrometer data to map mineralogy in the Rodalquilar caldera, southeast Spain," *International Journal of Remote Sensing*, vol. 30, no. 2, pp. 327–348, 2009.

[11] Christopher Kratt, Wendy M. Calvin, and Mark F. Coolbaugh, "Mineral mapping in the Pyramid Lake basin: Hydrothermal alteration, chemical precipitates and geothermal energy potential," *Remote Sensing of Environment*, vol. 114, no. 10, pp. 2297–2304, 2010.

[12] M. Mathieu, R. Roy, P. Launeau, M. Cathelineau, and D. Quirt, "Alteration Mapping on drill cores using HySpex SWIR-320m hyperspectral camera: application to the exploration of an unconformity-related uranium deposit (Saskatchewan, Canada)," *Journal of Geochemical Exploration*, vol. 172, pp. 71–88, 2017.

[13] Pedram Ghamisi, Javier Plaza, Yushi Chen, Jun Li, and Antonio J. Plaza, "Advanced Spectral Classifiers for Hyperspectral Images: A review," *IEEE Geoscience and Remote Sensing Magazine*, vol. 5, no. 1, pp. 8–32, 2017.

[14] B. Schölkopf and A. J. Smola, "Learning with Kernels," *Cambridge, MA: MIT Press*, 2002.

[15] L Breiman, "Random Forest," *Machine Leaming*, vol. 45, no. 1, pp. 5–32, 2001.

[16] C. Bishop, *Pattern Recognition and Machine Learning*, NY: Springer-Verlag, New York, 2006.

[17] G. Huang, S. Song, J. N.D. Gupta, and C. Wu, "Semi-supervised and unsupervised extreme learning machines," *IEEE Transactions on Cybernetics*, vol. 44, no. 12, pp. 2405–2417, 2014.

[18] G.-B Huang, Q.-Y. Zhu, and C.-K Siew, "Extreme Learning Machine : A New Learning Scheme of Feedforward Neural Networks," *IEEE International Joint Conference on Neural Networks*, vol. 2, pp. 985–990, 2004.

[19] V. Rodriguez-Galiano, M. Sanchez-Castillo, M. Chica-Olmo, and M. Chica-Rivas, "Machine learning predictive models for mineral prospectivity: An evaluation of neural networks, random forest, regression trees and support vector machines," *Ore Geology Reviews*, vol. 71, pp. 804–818, 2015.

[20] G.B Huang, Q.-Y. Zhu, and C.-k. Siew, "Extreme learning machine: theory and applications," *Neurocomputing*, vol. 70, no. 1, pp. 489–501, 2006.

[21] S. Jakob, R. Zimmermann, and R. Gloaguen, "The Need for Accurate Geometric and Radiometric Corrections of Drone-Borne Hyperspectral Data for Mineral Exploration: MEPHySTo-A Toolbox for Pre-Processing Drone-Borne Hyperspectral Data," *Remote Sensing*, vol. 9, no. 1, 2017.

[22] D. L. Whitney and B. W. Evans, "Abbreviations for names of rock-forming minerals," *American Mineralogist*, vol. 95, no. 1, pp. 185–187, 2010.